

SUPPLEMENTAL DATA TO**Humoral immunogenicity of the seasonal influenza vaccine
before and after CAR-T-cell therapy: a prospective observational study****TABLE OF CONTENTS**

SUPPLEMENTAL METHODS.....	2
Specimens	2
Laboratory testing.....	2
Neutralization assay.....	2
Hemagglutination inhibition (HAI) assay.....	3
Flow cytometry for B- and T-cells.....	4
Total immunoglobulins	5
Supplemental Analyses.....	5
SUPPLEMENTAL RESULTS.....	6
Correlation between the neutralization and the HAI assay.....	6
SUPPLEMENTAL FIGURES.....	7
Supplemental Figure 1. Vaccine administration and sample collection timelines.....	7
Supplemental Figure 2. Antibody titer fold-changes by baseline variables.....	8
SUPPLEMENTAL TABLES.....	9
Supplemental Table 1. Additional baseline demographics and clinical characteristics of the pre- and post-CAR-T-cell therapy cohorts	9
Supplemental Table 2. Baseline laboratory values and most recent IGRT administration for the pre- and post-CAR-T-cell therapy cohorts.....	11
REFERENCES	12

SUPPLEMENTAL METHODS

Specimens

Serum was isolated from whole blood collected in clot activator red top vacutainers and stored at -80°C. Peripheral blood mononuclear cells (PBMCs) were isolated by Ficoll Histopaque centrifugation from whole blood collected in acid citrate dextrose vacutainers, washed twice with phosphate-buffered saline, resuspended in a mixture of 90% fetal bovine serum and 10% dimethyl sulfoxide (DMSO), cooled at a controlled rate and stored in liquid nitrogen.

Laboratory testing

Laboratory work was blinded to clinical characteristics.

Neutralization assay

We used previously described fluorescent-based neutralization assays to measure neutralization against virus containing the H1 sequence derived from the A/Brisbane/2/2018 H1N1pdm09 virus strain.[1–3] To generate the viruses, a co-culture of 293T-PB1 cells and MDCK-SIAT1-TMPRSS2-PB1 cells were transfected with reverse-genetics plasmids which encoded the viral genomic segments, including a modified segment which included green fluorescent protein(GFP) in place of PB1 (encoded in a pHH-PB1flank-GFP plasmid), and a protein expression plasmid encoding TMPRSS2. We used the H1 protein sequence derived from the A/Brisbane/02/2018 (H1N1) virus strain (GISAID Accession EPI1671767, thanks to WHO Collaborating Centre for Reference and Research on Influenza). Other viral genes (PB2, PA, NP, NS, M, and NA) were derived from the A/WSN/1933 strain (kindly provided by Robert Webster of St. Jude Children's Research Hospital). The virus containing culture supernatants were clarified, aliquoted and frozen at -80°C. Prior to running neutralization assays, sera were treated with receptor-destroying enzyme (RDE) to prevent virus from binding to residual sialic

acids present in the serum. To do this, a vial of lyophilized RDE II (Seiken, Cat No. 370013) was resuspended in 20 mL PBS, then serum was diluted 1:4 into RDE solution, incubated at 37°C for 2.5 hr, and then heat-inactivated by incubating at 55°C for 30 min. In replicate dilution columns for each serum, RDE-treated sera were diluted down the columns of 96-well plate in neutralization assay medium (Medium 199 supplemented with 0.01% heat-inactivated FBS, 0.3% BSA, 100 U of penicillin/ml, 100 µg of streptomycin/ml, 100 µg of calcium chloride/ml, and 25 mM HEPES). Plates were incubated at 37°C for 1 hour to allow virus-antibody binding. Then, 5×10^4 MDCK-SIAT1-CMV-PB1 cells were added to each well. The cells enabled the virus to express GFP upon infection. Wells without added serum were used to measure maximal infectivity in the absence of neutralization. Wells without cells were used to measure background fluorescence in viral supernatants. After 16-20 hours incubation at 37°C, GFP fluorescence intensity was measured using an excitation wavelength of 485 nm and an emission wavelength of 515 nm (12-nm slit widths). Percent of maximal infectivity was calculated by subtracting background fluorescence signal from all wells and dividing the signal from serum-containing wells by the signal from corresponding wells without serum. Average infectivity over duplicate measurements were calculated. Curves of fluorescence intensity were plotted and the half maximal inhibitory concentrations (IC₅₀) were calculated using the *neutcurve* Python package (<https://jbloombio.github.io/neutcurve/>, 0.3.1). The IC₅₀ is defined as the dilution of serum needed to inhibit infectivity of virus by 50% of its maximum infectivity as measured when no antibodies are present. We reported the reciprocal of the IC₅₀ as the neutralization titer.

Hemagglutination inhibition (HAI) assay

HAI assays were performed to all four vaccine strains (FR-1665, FR-1666, FR-1667, FR-1669, International Reagent Resource, Manassas, VA). Serum samples were treated with RDE (VWR, Radnor, PE: MSPP370013) overnight at 37° and subsequently heated at 56°C for 30

minutes to remove nonspecific inhibitors. Serum was then adsorbed with red blood cells to remove nonspecific agglutinins. We prepared two replicate serial 2-fold dilutions (starting from 1:10) of 50 μ L of each treated sample on a 96-well microtiter plate, added 25 μ L standardized concentrations of vaccine antigen, and incubated at room temperature for 15 minutes. We added 50 μ L standardized turkey red blood cells to all wells and allowed to settle at room temperature for 30 minutes prior to result assessment. All runs included antisera and positive and negative controls. We reported the reciprocal of the highest dilution of serum that caused complete inhibition of hemagglutination as the HAI titer.

Flow cytometry for B- and T-cells

B-cells and T-cells were quantified using a research flow cytometry panel. Peripheral blood mononuclear cells (PBMCs) were incubated for 30 minutes on ice with antibodies contained in 100 μ L of FACS buffer that consisted of 1x DPBS containing 1% newborn calf serum (Life Technologies). Cells were then washed and analysed on a FACSymphony (BD Bioscience). The following antibodies were included for cell labelling: fixable viability dye (FV), anti-CD45 BV510 (HI30, BD), anti-CD3 BV605 (UCHT1, BioLegend), anti-CD4 Alexa Fluor 488 (OKT4, BioLegend), anti-CD8 APC-H7 (SK1, BD), anti-CD16 BV711 (3G8, BD), anti-CD14 BV711 (M0P-9, BD), anti-CD38 BUV661 (HIT2, BD), anti-IgD BUV737 (IA6-2, BD), anti-IgM PerCP- Cy5.5 (G20-127, BD), anti-CD20 BUV395 (2H7, BD), anti-CD19 BV421 (HIB19, BD), anti-CD27 PE-Cy7 (LG.7F9, Thermo Fisher), and anti-EGFR APC (cetuximab, R&D Systems). Naïve B-cells (CD19⁺CD27⁻CD38⁻IgD⁺) and switched memory B-cells (CD19⁺CD27⁺IgD⁻) were delineated within the lymphocyte population. Analyses were performed using FlowJo™ Software version 10.7.1 (Ashland, OR). Proportions from flow cytometry were multiplied with absolute lymphocyte counts from complete blood cell count results to calculate absolute B- and T-cell counts.

Total immunoglobulins

Total serum IgA, IgM, and IgG were measured using turbidometry (University of Washington Immunology Laboratory, Seattle, WA). In individuals with IgG MM, total functional IgG was estimated by subtracting the monoclonal component from the gamma region of serum protein electrophoresis

Supplemental Analyses

We used Spearman's correlation to determine the correlation between the neutralization and the HAI assays for the H1N1 vaccine strain.

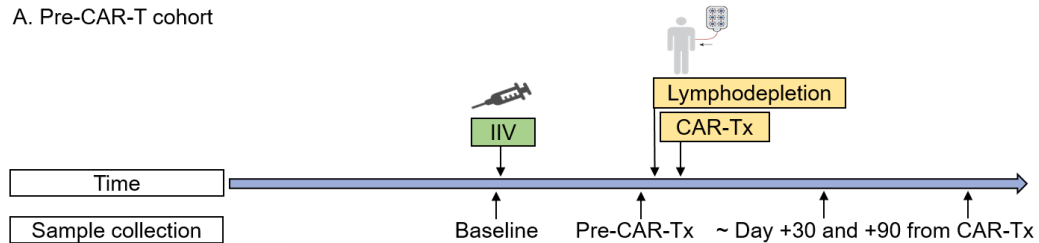
SUPPLEMENTAL RESULTS

Correlation between the neutralization and the HAI assay

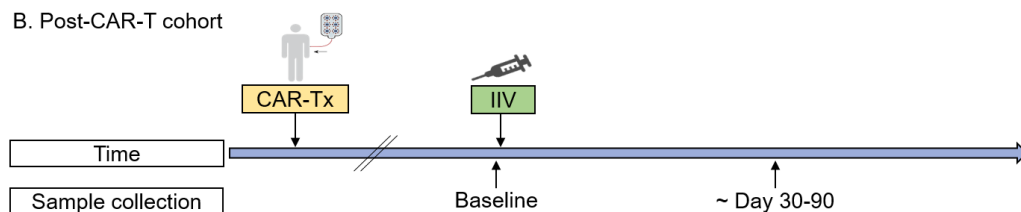
There was a good correlation between antibody titers for the neutralization assay and the HAI assay to A(H1N1) (baseline, $r=0.85$; first post-vaccine time point, $r=0.92$; fold-changes between baseline and the first post-vaccine time point, $r=0.64$). The neutralization assay was more sensitive with fewer titers below the limit of detection.

SUPPLEMENTAL FIGURES

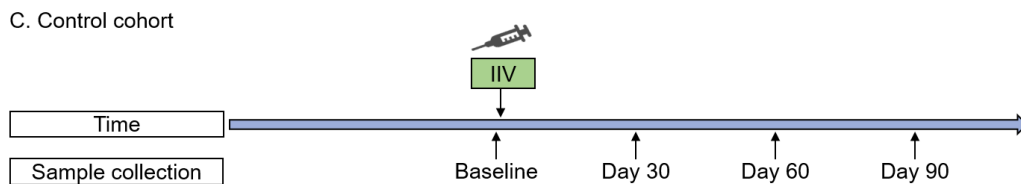
A. Pre-CAR-T cohort



B. Post-CAR-T cohort

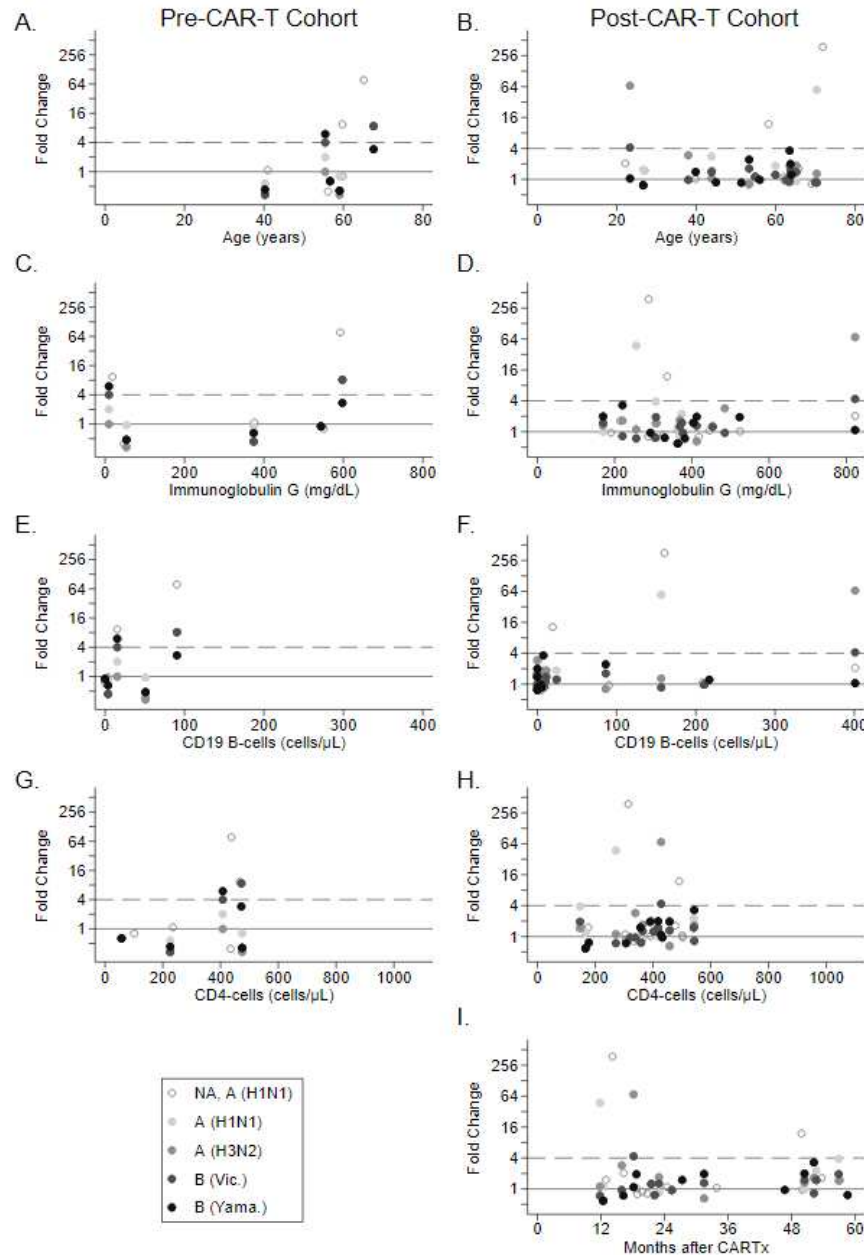


C. Control cohort

**Supplemental Figure 1. Vaccine administration and sample collection timelines.**

Timelines demonstrating blood sample collection, inactivated influenza vaccine (IIV) administration, and CAR-T-cell therapy (CAR-Tx) for the **(A)** pre-CAR-T cohort, **(B)** post-CAR-T cohort, and **(C)** control cohort.

Lymphodepletion indicates lymphodepleting chemotherapy.



Supplemental Figure 2. Antibody titer fold-changes by baseline variables

Antibody titer fold-changes from baseline to the first post-vaccine time point are depicted by baseline variables of interest in the pre-CAR-T cohort (panels in the left column, $n=5$) and the post-CAR-T cohort (panels in the right column, $n=13$). Baseline variables are: (A, B) Age, (C, D) immunoglobulin G (lower limit of normal [LON], 610 mg/dL), (E, F) CD19⁺ B-cell count (lower LON, 100 cells/ μ L), (G, H) CD4⁺ T-cell count (lower LON, 500 cells/ μ L), and (I) months after CAR-T-cell therapy (CAR-Tx) in the post-CAR-T cohort only. For each individual, results from each vaccine strain and test type are presented and indicated in the figure legend. NA indicates neutralization assay; other results are based on HAI assays. A fold-change of 1 (solid horizontal line) indicates no change in antibody titer from baseline. Symbols on or above the upper dashed horizontal line represent ≥ 4 fold-changes.

SUPPLEMENTAL TABLES

Supplemental Table 1. Additional baseline demographics and clinical characteristics of the pre- and post-CAR-T-cell therapy cohorts

		Pre-CAR-T cohort		CAR-T-cell therapy		Pre-CAR-T cohort		Post-CAR-T cohort ^d	Vaccine	
Study ID	Treatment lines before CAR-Tx, n	Last treatment line before CAR-Tx	Days from last treatment to vaccine	CAR-Tx product or study protocol number ^a	Co-stimulatory domain	Treatment for immune related adverse events ^b	Disease status 90d post CAR-Tx	Treatments in the 6 months prior to vaccination	Vaccine name, manufacturer	Vaccine type
Pre-CAR-T cohort										
Individuals with an antibody response to ≥1 vaccine strain										
Pre-4	6	Daratumumab, pomalidomide, dexamethasone	35	NCT03338972	4-1BB	Corticosteroids, tocilizumab	VGPR		Fluarix, GSK	split
Pre-5	9	Daratumumab, bortezomib, dexamethasone	112	NCT03338972	4-1BB	Corticosteroids	VGPR		Fluarix, GSK	split
Individuals without antibody responses										
Pre-1	2	Blinatumomab	35	NCT03103971	4-1BB	Corticosteroids, tocilizumab	CR ^c		Fluarix, GSK	split
Pre-2	8	Lenalidomide	50	NCT03277729	CD28 and 4-1BB		Persistent		Fluarix, GSK	split
Pre-3	11	Carfilzomib, cyclophosphamide, thalidomide, dexamethasone	35	NCT03502577	4-1BB		Progressive ^e		Fluarix, GSK	split
Post-CAR-T cohort										
Individuals with an antibody response to ≥1 vaccine strain										
Post-1	8			NCT02028455	4-1BB				Fluzone, Sanofi	split
Post-4	5			NCT01865617	4-1BB				Flucelvax, Seqirus	Surface antigen/cell based
Post-11	3			NCT01865617	4-1BB				Flucelvax, Seqirus	Surface antigen/cell based
Post-13	14			NCT03338972	4-1BB				Fluad, Seqirus	Subunit/adjuvant
Individuals without antibody responses										
Post-2	7			NCT02028455	4-1BB				Flucelvax, Seqirus	Surface antigen/cell based
Post-3	7			NCT01865617	4-1BB			Ruxolitinib for GvHD	NK	NK
Post-5	7			NCT01865617	4-1BB				FluLaval, GSK	split

Post-6	5			NCT01865617	4-1BB			Ibrutinib ^e	Fluzone, high dose, Sanofi	split
Post-7	3			Axicabtagene ciloleucel NCT03105336	CD28				Fluarix, GSK	split
Post-8	2			Axicabtagene ciloleucel	CD28				Fluzone, Sanofi	split
Post-9	4			NCT01865617	4-1BB				FluLaval, GSK	split
Post-10	5			Lisocabtagene maraleucel NCT02631044	4-1BB				Fluzone, Sanofi	split
Post-12	3			Axicabtagene ciloleucel	CD28				NK	NK

Blank fields indicate not applicable. NK indicates not known. Baseline is defined as the day of the baseline blood sample prior to vaccination.

CAR-Tx indicates CAR-T-cell therapy; GSK, GlaxoSmithKline; GvHD, graft versus host disease; NK, not known.

^aAll individuals received a standard lymphodepleting regimen with cyclophosphamide and fludarabine.

^bIncludes cytokine release syndrome and immune effector cell-associated neurotoxicity syndrome.

^c'Pre-1' had an allogeneic HCT prior to day 90 for consolidation; 'Pre-3' died prior to the 90 day time point.

^dAll individuals had remission or very good partial remission of the underlying disease at time of vaccination without initiation of new therapies after CAR-T-cell therapy.

^eMaintenance therapy started before CAR-T-cell therapy.

Supplemental Table 2. Baseline laboratory values and most recent IGRT administration for the pre- and post-CAR-T-cell therapy cohorts

Study-ID	CD8 ⁺ T-cells/ μ L	% naïve of all CD19 ⁺ B-cells ^a	% switched memory of all CD19 ⁺ B-cells ^a	IgA, mg/dL ^b	IgM, mg/dL ^b	Days from last IGRT to baseline ^c	Days from last IGRT to post vaccine timepoint ^c
Pre-CAR-T cohort							
Individuals with an antibody response to \geq1 vaccine strain							
Pre-4	359	41	33	5	<10		
Pre-5	801	52	8	21	24		
Individuals without antibody responses							
Pre-1	224			38	<10		
Pre-2	399			67	27		
Pre-3	217	29	4	<2	<10		
Post-CAR-T cohort							
Individuals with an antibody response to \geq1 vaccine strain							
Post-1	759	47	2	7	126		
Post-4	262			3	21		
Post-11	138			14	10		
Post-13	189	63	2	59	223		
Individuals without antibody responses							
Post-2	147			2	10	66	71
Post-3	104			3	10	95	43
Post-5	223			3	10		
Post-6	401			34	10		
Post-7	531			37	19		
Post-8	247			33	10	62	
Post-9	346	64	2	2	34		
Post-10	181	79	1	53	18		
Post-12	167			37	10		
IGRT indicated IgG replacement therapy.							
^a No values are missing. Percentage of B-cell subpopulations are only displayed among individuals with \geq 20 CD19 ⁺ B-cells/ μ L.							
^b Lower limits of normal; IgA, 84 mg/dL; IgM, 40 mg/dL.							
^c IGRT within 4 months (\geq 4 half-lives of circulating IgG) before any of the study sample collections is displayed. IGRT within 2 months prior to baseline was an exclusion criteria.							

REFERENCES

- 1 Doud MB, Hensley SE, Bloom JD. Complete mapping of viral escape from neutralizing antibodies. *PLoS Pathog* 2017;**13**:e1006271. doi:10.1371/journal.ppat.1006271
- 2 Hooper KA, Bloom JD. A mutant influenza virus that uses an N1 neuraminidase as the receptor-binding protein. *J Virol* 2013;**87**:12531–40. doi:10.1128/JVI.01889-13
- 3 Lee JM, Eguia R, Zost SJ, *et al.* Mapping person-to-person variation in viral mutations that escape polyclonal serum targeting influenza hemagglutinin. *Elife* 2019;**8**. doi:10.7554/ELIFE.49324